

Investigation on Structural and Luminescence Properties of Dy³⁺ - ions Doped Bismuth Borate Glasses for Optoelectronic Devices

B. Munisudhakar¹, C. Nageswara Raju^{2*}, M. Reddi Babu³,
A. Mohan Babu³, L. Rama Moorthy³ and N. Manohar Reddy⁴

¹Research Scholar, JNTUA,
Ananthapuramu, India-515 002

^{2*}Department of Physics, Sri Venkateswara Degree College,
Kadapa, India-516003

³Department of Physics, Chadalawada Ramanamma Engineering College,
Tirupati, India-517506

⁴Department of Physics, Sri Venkateswara College of Engineering,
Tirupati, India-517502

Abstract

Dy³⁺ ions doped bismuth borate glasses of chemical composition 5Bi₂O₃-(65-x) B₂O₃-10ZnO-10Pb₃O₄-10AlF₃-xDy₂O₃ (where x=0.0, 0.1, 0.5, 1.0, 2.0 and 3.0mol %) were prepared by the melt quenching technique and investigated through X-ray diffraction, SEM, FTIR, absorption, luminescence emission and decay studies. From XRD, SEM and FTIR structural characterization was accomplished. The luminescence properties were analyzed using absorption, excitation, photoluminescence and decay studies. From absorption spectrum, the Judd-Ofelt intensity parameters (Ω_λ , $\lambda = 2, 4$ and 6) were evaluated and are in turn used to determine the radiative parameters such as branching ratios (β_R), radiative transition probabilities (A_R), effective band width ($\Delta\lambda_{exp}$), stimulated emission cross-sections (σ_e), for the excited ⁴F_{9/2} level of Dy³⁺ ions. The non exponential nature of decay curves of the excited ⁴F_{9/2} level of Dy³⁺ ions in all glasses were analyzed. From all the results, it is observed that 1 mol % Dy³⁺ doped BBZPA glasses are suitable for optoelectronic devices such as for lasers and white LEDs.

Keywords: Bismuth borate glasses, Dysprosium, Judd-Ofelt analysis, Photoluminescence, Radiative parameters.

1. Introduction

In recent years, an extensive research is focused on the investigation of the rare earth (RE) ions doped glasses due to their potential applications in the designing of several optical devices such as optical memory devices, flat panel devices, magneto-optical devices, wave-guide devices, display devices, solid state lasers, up conversion lasers, fibre lasers, medical lasers, eye safe lasers, compact micro-chip lasers, Q-switching of lasers, fibre amplifiers, fluorescent lamps, solar concentrators, glass scintillators, white LED's and sensors etc [1-3].

Among the different oxide glass hosts such as silicate, germanate, phosphate and tellurite glasses, the borate glasses are the most suitable ones for optical devices due to their high transparency, low melting point, high thermal stability, low refractive index and low dispersion, high solubility for rare earth (RE) ions and these glasses possess a high phonon energies (1300 cm⁻¹) due to stretching vibrations of network forming oxides [4,5]. Recently, it has been observed that the phonon energies of these glass hosts can be reduced by the addition of suitable heavy metal oxides (HMO) like PbO, Bi₂O₃, Al₂O₃, MoO₃ and WO₃ etc [6,7]. Consequently, increase in the quantum efficiency of luminescence from excited states of rare earth ions.

Among trivalent rare earth [RE³⁺] ions, the Dy³⁺ (4f⁹) ion has been considered as promising candidates for analyzing the luminescence properties because its 4f-4f transitions exhibit higher quantum efficiency.

The luminescence spectrum of Dy³⁺ ion, consists of 4F_{9/2} → 6H_j (j = 7/2, 9/2, 11/2, 13/2, and 15/2) transitions, in the visible and infrared regions. In the visible region, Dy³⁺ ion exhibits two predominant intense emission bands at yellow (570-600 nm) and blue (470-500 nm) corresponding to the ⁴F_{9/2} → ⁶H_{13/2} and ⁴F_{9/2} → ⁶H_{15/2} transitions due to the electric dipole transition and magnetic dipole transitions. Additionally, the intensity of ⁴F_{9/2} → ⁶H_{13/2} (yellow) transition of Dy³⁺ ions is hypersensitive (ΔL = 2 and ΔJ = 2) and its intensity strongly depends on the nature of the host material, where as the ⁴F_{9/2} → ⁶H_{15/2} (blue) transition is less sensitive to the host material [8,9]. The luminescence intensity ratio (Y/B) is the relative intensity of the ⁴F_{9/2} → ⁶H_{13/2} (yellow) transition to the ⁴F_{9/2} → ⁶H_{15/2} (blue) transition which measures the local symmetry in the environment of Dy³⁺ ions. At suitable environment, yellow to blue (Y/B) intensity ratio will change and Dy³⁺ ions will emit white light.

Thus, the Dy³⁺ - doped luminescent materials are used to obtain two primary colours in glasses as well as white light both in glasses and phosphors [10]. Recently, K. Siva Rama Krishna Reddy et al. [11] reported investigation on structural and luminescence of features of Dy³⁺ ions doped alkaline-earth boro tellurite glasses for optoelectronic devices. Spectroscopy and energy transfer in lead borate glasses doubly doped with Tm³⁺ and Dy³⁺ ions were studied by Agata Gorny et al. [12]. Physical and structural studies on magnesium borate glasses doped with dysprosium ion were reported by A. Ichoja et al. [13]. Spectroscopic investigations on Dy³⁺ ions doped zinc lead alumina borate glasses for photonic device application were studied by Nisha Deopa et al. [14] have made a systematic study on structural and luminescence properties of Dy³⁺ - ions doped borate glasses.

In this present work, bismuth borate glass Dy³⁺ doped with various concentrations were prepared by melt quenching method and is to investigate the physical, structural, optical absorption, luminescence and decay properties of the ⁴F_{9/2} → ⁶H_{13/2} transition level for lasers and white LEDs.

2. Experimental details

2.1. Preparation of Glasses

Dy³⁺ doped bismuth borate (BBZPA) glasses were prepared by the traditional melt quenching method with a glass composition of 5Bi₂O₃ - (65-x)B₂O₃ - 10ZnO - 10Pb₃O₄ - 10AlF₃ - xDy₂O₃ where x = 0, 0.1, 0.5, 1.0 2.0 and 3.0

(in mol %) and referred as BBZPADy0.0, BBZPADy0.1, BBZPADy0.5, BBZPADy1.0, BBZPADy2.0, and BBZPADy3.0, respectively and are presented in Table 1.

The glass composition of 15 g batches with high purity (99.99%) Bi₂O₃, B₂O₃, ZnO, Pb₃O₄, AlF₃ and Dy₂O₃ chemicals were mixed and crushed in agate mortar and this homogeneous mixture was taken into a alumina crucible and melted in an electric furnace at 1200 °C for 1 hour. After melting, glass melts were poured into a preheated brass mould for quenching and annealed at 350 °C for 15 hours to remove the thermal strains and polished for physical, structural and luminescence properties.

Glass code	Glass composition (mol %)
BBZPA Dy0.0	65-B ₂ O ₃ -10Pb ₃ O ₄ -5Bi ₂ O ₃ -10ZnO-10AlF ₃
BBZPA Dy0.1	64.9-B ₂ O ₃ -10Pb ₃ O ₄ -5Bi ₂ O ₃ -10ZnO-10AlF ₃ -0.5Dy ₂ O ₃
BBZPA Dy0.5	64.5-B ₂ O ₃ -10Pb ₃ O ₄ -5Bi ₂ O ₃ -10ZnO-10AlF ₃ -0.1 Dy ₂ O ₃
BBZPA Dy1.0	64-B ₂ O ₃ -10Pb ₃ O ₄ -5Bi ₂ O ₃ -10ZnO-10AlF ₃ -1.0 Dy ₂ O ₃
BBZPADy2.0	63-B ₂ O ₃ -10Pb ₃ O ₄ -5Bi ₂ O ₃ -10ZnO-10AlF ₃ -2.0 Dy ₂ O ₃
BBZPADy3.0	62-B ₂ O ₃ -10Pb ₃ O ₄ -5Bi ₂ O ₃ -10ZnO-10AlF ₃ -3.0 Dy ₂ O ₃

Table 1 Chemical composition of the Dy³⁺ - doped BBZPA glasses.

2.2. Characterization techniques

The physical parameters such as refractive index (1.652) of BBZPADy1.0 glass was measured ~ at 30 °C using an Abbe's refractometer ATAGO of sodium wavelength 589.3 nm of accuracy up to ±0.0002 with mono bromonaphthalene (C₁₀H₇Br) as an adhesive coating and density (4.52 g/cm³) was determined by the Archimedes method using distilled water as an immersion liquid. The X-ray diffraction spectrum for the prepared BBZPADy1.0 glass was recorded by using X-ray diffractometer (Seifert; Model 30003TT) with Cu K_α radiation Source. The SEM micrograph of BBZPADy0.0 was recorded. Four transform infrared spectrum (FTIR) for BBZPADy0.0 glass was recorded on the Perkin Elmer IR spectrometer in the region 400-4000 cm⁻¹. The absorption spectrum of BBZPADy1.0 was recorded in the wavelength 400 - 1000 nm using a JASCO V-770 UV-VIS-NIR spectrophotometer. The PL spectra and decay profile measurements of the prepared glasses were measured using Edinburgh FLS-980 fluorescence spectrometer at room temperature.

3. Results and discussion

3.1. Physical properties

Physical properties of prepared BBZPADy1.0 glass was calculated and presented in Table 2.

Table 2 Physical properties of BBZPADy1.0 glass.

Physical properties	BBZPADy1.0
Refractive index (n)	1.652
Density (g/ cm ³)	4.52
Molecular weight (M) g/mol	156.68
Dy ³⁺ ion concentration (mol/lit)	0.288
Dy ³⁺ ion concentration (10 ²⁰ ions/ cm ³)	1.73
Molar volume (V _m) cm ³ /mol	34.66
Molar refractivity (R _m) cm ³	12.672
Molar electronic polarizability (α _m) in 10 ⁻²⁴ cm ³ /mol	5.028
Reflection losses (R) in %	5.76
Dielectric constant (ε)	2.729
Optical dielectric constant (ε - 1)	1.729
Metallization factor (M)	0.634
Numerical aperture (NA)	0.233

3.2. Structural analysis

3.2.1. XRD and SEM analysis

Fig.1 shows the XRD spectrum of BBZPADy1.0 glass and indicates the absence of no sharp Bragg's speaks, but only a broad diffuse hump around low angle region which confirms the amorphous nature of the prepared glass.

Fig.2 shows the smooth surface without presence of grains, which confirms the amorphous as well as the homogeneous nature of the prepared glass sample.

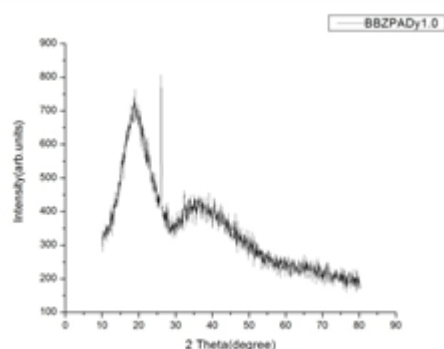


Fig. 1 XRD spectrum of BBZPADy1.0 glass

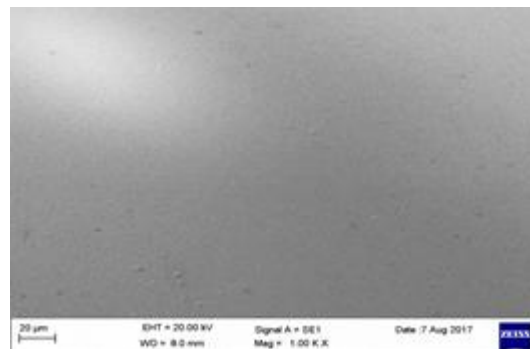


Fig. 2 SEM micrograph of BBZPADy0.0 glass

3.2.2. FTIR spectrum

FTIR spectrum of BBZPADy0.0 glass was recorded in the wave number region of 400-4000 cm⁻¹ as shown in Fig. 3 and the corresponding band assignments are tabulated in Table 3. The present glass shows transmission bands in regions 2339, 2114, 1874, 1201, 867 and 692 cm⁻¹ [15-16]. It has been observed that the bands observed in the region 2339-2114 cm⁻¹ are due to the OH bending mode of vibration. The band around 1874 cm⁻¹ is due to the crystal water with H-O-H bending mode. The band around 1201 cm⁻¹ is due to the Asymmetric stretching vibrations of B-O bonds in BO₃ and B₂O₇ units. The band around 867 cm⁻¹ is due to the stretching vibration of BO⁴ in diborate group. The band around 692 cm⁻¹ is due to the B-O-B linkage bending vibrations in borate network.

Table 3 FTIR Spectral bands and their assignments for BBZPADy0.0 glass.

BBZPADy1.0	Assignments
2114-2339	OH bending mode of vibration
1784-1874	Crystal water with H-O-H bending mode
1201	Asymmetric stretching vibrations of B-O bonds in BO ₃ and B ₂ O ₇ units
867	Stretching vibration of BO ⁴ in diborate group
689	B-O-B linkage bending vibrations in borate network

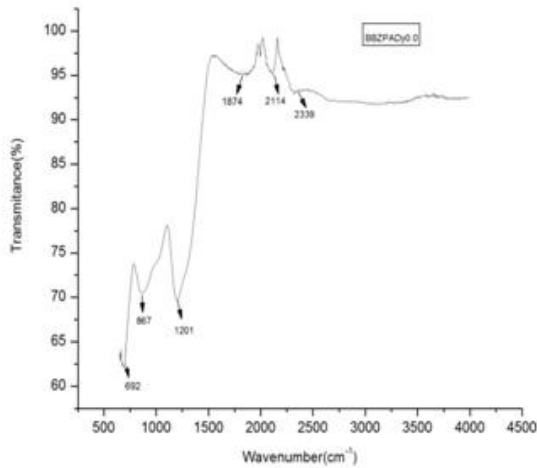


Fig.3 FTIR spectrum of BBZPADy0.0 glass

3.3. Optical absorption spectrum and J-O analysis

Fig.4 shows the typical absorption spectrum along with band assignment of BBZPADy1.0 glass recorded in the 300 -1800 nm region.

The absorption spectra for the remaining Dy³⁺ doped BBZPA glasses are also quite similar in the peak positions expect some variations in their peak intensities and hence not shown here. Each absorption spectrum consists of eleven absorption bands that are located at 362, 410, 425, 453, 472, 750, 800, 898, 1088, 1269 and 1673 nm which are assigned to ⁶H_{15/2} → ⁶P_{5/2}, ⁴I_{13/2}, ⁴G_{11/2}, ⁴I_{15/2}, ⁴F_{9/2}, ⁶F_{3/2}, ⁶F_{5/2}, ⁶F_{7/2}, ⁶F_{9/2}, ⁶F_{11/2} and ⁶H_{11/2} transitions respectively. The assignment of absorption transitions has been made according to the earlier studied Dy³⁺ ions doped glasses [17].

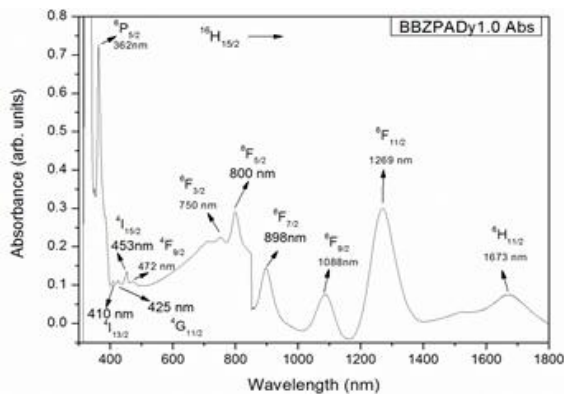


Fig.4 Absorption spectrum of BBZPADy1.0 glass in UV-visible and NIR regions.

Among all transitions of Dy³⁺ ions, the transition ⁶H_{15/2} → ⁶F_{11/2} transition located at 1269 nm shows higher intensity compared to the other transitions and obey the selection rules $|\Delta L| \leq 0, |\Delta J| \leq 0, |\Delta S|=0$ and hence they are known as hypersensitive transitions.

Using absorption spectrum, the experimental oscillator strengths (f_{exp}) can be evaluated by measuring the integrated area under the absorption band using the following equation [18].

$$f_{exp} = 4.32 \times 10^{-9} \int \epsilon(\nu) d\nu \quad (1)$$

where $\epsilon(\nu)$ is the molar absorptivity of a band at a wavenumber ν (cm⁻¹).

According to JO theory [19- 21], the theoretical oscillator strengths (f_{cal}) for absorption bands corresponding to the electron dipole f-f transition from the initial state ψJ to final state $\psi' J'$ can be calculated by using following equation.

$$f_{cal}(\Psi J, \Psi' J') = \frac{8\pi^2 m c \nu}{3h(2J+1)} \left[\frac{(n^2+2)^2}{9n} S_{ed}(\Psi J, \Psi' J') + n S_{md}(\Psi J, \Psi' J') \right] \quad (2)$$

where h is the Planck's constant, m and e are mass and charge of an electron, c is the speed of light, n is refractive index of the medium, ν is the wave number, $(n^2 + 2)^2 / 9n$ is the Lorentz local field correction factor for the absorption band and (2J+1) is the degeneracy of the ground state ^{2S+1}L_J. The electric (S_{ed}) and magnetic (S_{md}) dipole dipole strengths are given by

$$S_{ed}(\Psi J, \Psi' J') = e^2 \sum_{\lambda=2,4,6} \Omega_{\lambda} \left\langle \Psi J \left\| U^{\lambda} \right\| \Psi' J' \right\rangle^2 \quad (3)$$

$$S_{md}(\Psi J, \Psi' J') = \frac{e^2 h^2}{16\pi^2 m^2 c^2} \left\langle \Psi J \left\| (L+2S) \right\| \Psi' J' \right\rangle^2 \quad (4)$$

where Ω_{λ} ($\lambda=2,4$ and 6) represents the J-O intensity parameters and $\|U^{\lambda}\|$ are the doubly reduced matrix elements. A standard least square fitting approximation is used to get good fit between the experimental (f_{exp}) and calculated (f_{cal}) oscillator strengths as well to determine the JO intensity parameters Ω_{λ} ($\lambda=2, 4$ and 6). The quality of fit between the f_{exp} and f_{cal} is expressed as the root mean square deviation (δ_{rms}) using the following relation.

$$\delta_{rms} = \left[\frac{\sum (f_{exp} - f_{cal})^2}{N} \right]^{\frac{1}{2}} \quad (5)$$

where 'N' is the total number of energy levels presenting in the fitting procedure. The experimental and calculated oscillator strengths for the BBZPADy1.0 glass are presented in Table 4. The obtained value of root mean square deviation (δ_{rms}) of $\pm 0.68 \times 10^{-6}$, indicates the best fit between the experimental and calculated oscillator strengths.

Table 4 Observed band positions λ_p (cm), energies (cm⁻¹), experimental ($f_{exp} \times 10^{-6}$), calculated ($f_{cal} \times 10^{-6}$) oscillator strengths and root mean square deviation ($\delta_{rms} \times 10^{-6}$) of BBZPADy1.0 glass

Transition from ground state $6H_{15/2}$	Wavelength h(nm)	Energy(cm ⁻¹)	Oscillator strengths	
			f_{exp}	f_{cal}
${}^6H_{11/2}$	1673	5977	0.63	1.29
${}^6F_{11/2}$	1269	7880	5.64	5.54
${}^6F_{9/2}$	1088	9191	1.57	1.92
${}^6F_{7/2}$	898	1123	3.54	1.99
${}^6F_{5/2}$	800	1250	0.65	1.02
${}^6F_{3/2}$	750	1333	0.06	0.19
${}^4F_{9/2}$	472	2118	0.08	0.15
${}^4I_{15/2}$	453	2207	0.24	0.46
${}^4G_{11/2}$	425	2352	0.1	0.31
${}^4I_{13/2}$	410	2439	0.1	0.3
${}^6P_{3/2}$	362	2762	5.1	2.46
			$\delta_{rms} =$	
			\pm	0.68

The estimated values of J-O intensity parameters for the BBZPADy1.0 glass are tabulated in Table 5 and the values compared with different host glass materials [9, 11, 23].

From the Table 5, it is observed that the JO intensity parameters were found to be $\Omega_2 = 7.45 \times 10^{-20} \text{ cm}^2$, $\Omega_4 = 6.99 \times 10^{-20} \text{ cm}^2$ and $\Omega_6 = 2.57 \times 10^{-20} \text{ cm}^2$ and follows the trend $\Omega_2 > \Omega_4 > \Omega_6$ and spectroscopic quality factor is 0.68.

Table 5 Judd-Oflet (JO) intensity parameters ($\Omega_\lambda, \times 10^{-20} \text{ cm}^2$) for BBZPADy10 glass with other reported glasses.

Glass code	JO Parameters			Trends of Ω_λ
	Ω_2	Ω_4	Ω_6	
BBZPADy10 [Present Work]	7.45	6.99	2.57	$\Omega_2 > \Omega_4 > \Omega_6$
PKAZFDy [9]	14.11	3.07	1.95	$\Omega_2 > \Omega_4 > \Omega_6$
AEBT [11]	4.04	1.86	0.82	$\Omega_2 > \Omega_4 > \Omega_6$
Dy:LiLTB [23]	8.75	2.62	2.07	$\Omega_2 > \Omega_4 > \Omega_6$
Dy:NaLTB [23]	9.25	2.87	2.29	$\Omega_2 > \Omega_4 > \Omega_6$
Dy:KLTB [23]	9.86	3.39	2.41	$\Omega_2 > \Omega_4 > \Omega_6$

3.4. Luminescence spectra and Radiative properties

The excitation spectra of Dy³⁺-doped BBZPADy1.0 glass were recorded by monitoring emission at 574 nm wavelength in the spectral range from 300-550 nm is shown in Fig 5. The excitation spectrum consists of seven bands observed at 325, 351, 365, 387, 425, 453 and 472 nm corresponding transitions from ground state level ${}^6H_{15/2}$ to the excited states ${}^6P_{3/2}$, ${}^6P_{7/2}$, ${}^6P_{5/2}$, ${}^4K_{17/2}$, ${}^4G_{11/2}$, ${}^4I_{15/2}$ and ${}^4F_{9/2}$

respectively [22, 23]. Among these excitation bands, the excitation band at 387 nm (${}^6H_{15/2} \rightarrow {}^4K_{17/2}$) has high intensity and is used to record the emission spectra.

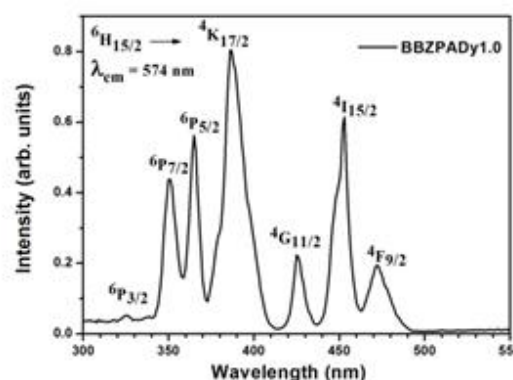


Fig.5 Photoluminescence Excitation spectrum of BBZPADy1.0 glass upon emission at 574 nm.

Photo luminescence spectra of Dy³⁺-doped BBZPADy1.0 glass were recorded in the spectral range of 400-700 nm by monitoring excitation at 387 nm wavelength is shown in Fig 6. From the spectra, it is observed that the emission spectra shows two strong luminescence bands and one weak band at 480, 574 and 663 nm which corresponds ${}^4F_{9/2} \rightarrow {}^6H_{15/2}$ (blue), ${}^4F_{9/2} \rightarrow {}^6H_{13/2}$ (yellow) and ${}^4F_{9/2} \rightarrow {}^6H_{11/2}$ (red) transitions respectively. The intensity of these emission bands is similar except in small variations.

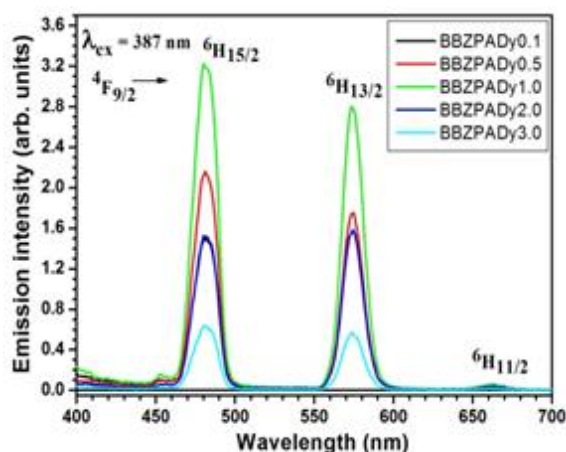


Fig.6 NIR emission spectra of BBZPADy (x = 0.0, 1.0, 0.5, 1.0, 2.0 and 3.0 mol %) glasses.

From the luminescence spectra, Peak positions (λ_p), branching ratios (β_R), effective band width ($\Delta\lambda_{exp}$) are determined and also the radiative parameters such as transition probabilities (A_R), radiative lifetimes (τ_R), and emission cross-sections (σ_e) for the $\Psi J \rightarrow \Psi' J'$ emission transitions have been determined and are presented in Table 6.

Table 6 Emission Peak positions (λ_p , nm), branching ratios (β_R), radiative transition probabilities (A_R, s^{-1}), effective bandwidth ($\Delta\lambda_{exp}$, nm), stimulated emission cross sections ($\sigma_e, \times 10^{-21} \text{ cm}^2$), values for ${}^4I_{13/2} \rightarrow {}^4I_{15/2}$ transition of the BBZPADy1.0 glass.

Transition from ${}^4F_{9/2}$	λ_p (nm)	Branching ratios		A_R	τ_{exp}	τ_R
		$\beta_{13/2}$	$\beta_{15/2}$			
${}^6H_{15/2}$	480	0.59	0.15	170	16.23	0.36
${}^6H_{13/2}$	574	0.45	0.69	1124	15.11	5.29
${}^6H_{11/2}$	663	0.01	0.07	142	14.10	1.23

In general, the branching ratio (β_R) characterizes the possibility of attaining stimulated emission from any specific direction and also it is a critical parameter to laser designer. In the present study, the values of branching ratio (β_R) and stimulated emission cross-section (σ_e) transition are found to be largest for ${}^4F_{9/2} \rightarrow {}^6H_{13/2}$ lasing transition.

These results suggest that this transition of BBZPADy1.0 glass might be suitable for laser emission in yellow region.

3.5. Luminescence decay analysis

Fig.7 shows the luminescence decay profiles of the ${}^4F_{9/2} \rightarrow {}^6H_{13/2}$ transition of the Dy^{3+} doped BBZPA glasses are recorded with an emission wavelength of 481 nm and monitored at 387 nm excitation. It is observed that the decay curves exhibit single exponential nature at lower Dy^{3+} concentrations (<1.0 mol %) and non exponential nature at higher Dy^{3+} concentrations (≥ 1.0 mol %). The experimental life time ($\tau_{exp} = 259 \mu s$) for ${}^4F_{9/2}$ excited level of Dy^{3+} ion in BBZPADy10 glass was found to be lower than the radiative lifetime ($\tau_R = 462 \mu s$) obtained from JO analysis.

The quantum efficiency (η) of the excited level can be obtained using the formula

$$\eta\% = \frac{\tau_{exp}}{\tau_R} \times 100\% \quad (6)$$

For BBZPADy1.0 glass, the value of η is found to be 56%. From the experimental results, it is suggested that the BBZPADy1.0 glass is more suitable for optoelectronic applications.

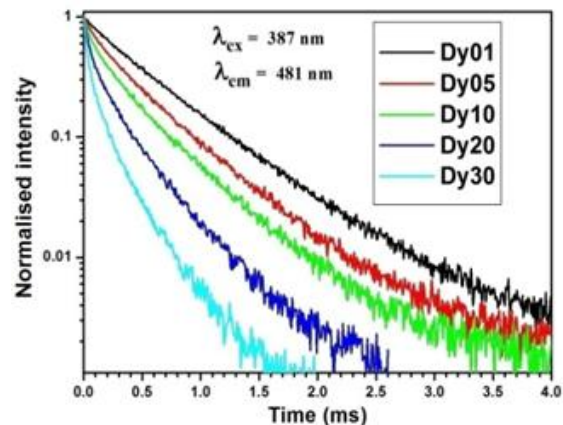


Fig.7 Fluorescence decay curves for ${}^6H_{15/2}$ excited state of BBZPADyx ($x = 0.0, 0.1, 0.5, 1.0, 2.0$ and 3.0 mol %) glasses upon excitation.

4. Conclusions

In the present investigated Dy^{3+} ions doped BBZPA glasses were prepared by using melt quenching technique. The XRD spectrum and SEM micrographs confirmed the amorphous nature of prepared glasses. The assignments of different structural groups were identified by using FTIR spectrum. Judd-Oflet analysis was carried out to evaluate intensity parameters in the order $\Omega_2 > \Omega_4 > \Omega_6$ and in turn to predict radiative parameters. The non exponential nature of decay curves of the excited ${}^4F_{9/2}$ level of Dy^{3+} ions in all glasses were analyzed. From the PL spectra, it is observed that the large stimulated emission cross-sections of the ${}^4F_{9/2} \rightarrow {}^6H_{13/2}$ transition suggest that the present BBZPADy1.0 glass is most suitable for yellow lasers as well as optical amplifiers. Based on the results, we observed that the BBZPADy1.0 glass is aptly suitable for optoelectronic devices.

References

- [1] K. Annapoorani, Ch. Basavapoornima, N. Surya, Murthy, K. Marimuthu, Investigations on structural and behavior of Er^{3+} doped Lithium Zinc borate glasses for lasers and optical amplifier applications, *J. Non-cryst. Solid.* 447(2016)273-282.
- [2] P.P. Pawar, S.R. Munishwar, R.S. Gedam, Physical and optical properties of Dy^{3+}/Pr^{3+} co-doped lithium borate glasses for W-LED, *Journal of Alloys and Compound* 660(2016)347-355.
- [3] S. Farooq, Y. Munikrishna Reddy, R. Padmasuvarna, Venkata Krishnaiah, C.S. Dwaraka Viswanath, Sk. Mahamu Structure and photoluminescence of dysprosium doped antimony – magnesium-strontium oxyfluoroborate glasses, *Ceramics International*, 2018.

- [4] I. Kashif, A. Abd El-Maboud, A. Ratep, Effect of Nd_2O_3 addition on structure and characterization of lead bismuth borate glass, *Results in Physics* 4 (214) 1 – 5.
- [5] G. Gupta, A.D. Sontakke, P. Karmakar, K. Biswas, S. Balaji, R. Saha, R. Sen, K. Annapurna, Influence of bismuth on structural, elastic and spectroscopic properties of Nd^{3+} doped zinc-boro-bismuthate glasses, *J. Lumin.* 149 (2014) 163 – 169.
- [6] Sk. Mahamuda, K. Swapna, A. Srinivasa Rao, M. Jayasimhadri, T. Sasikala, K. Pavani, L.Rama Moorthy, Spectroscopic properties and luminescence behavior of a Nd^{3+} doped zinc alumino bismuth borate glasses, *J. Phys. Chem. Solids* 74 (2013) 1308 – 1315.
- [7] S.Damodaraiah, V.ReddyPrasad, S.Babu, Y.C.Rathakaram, Structural and luminescence properties of Dy^{3+} doped bismuth phosphate glasses for greenish yellow light applications, *Optical Materials* 67(2017) 14-24.
- [8] P.Babu, Kyoung Hyuk Jang, Eun Sik Kim, Liang Shi, Hyo Jin Seo, F.Rivera-Lopez, U.R.Rodriguez-Mendoza, V.Lavin, R.Vijaya, C.K.Jayasankar, Spectral investigations on Dy^{3+} -doped transparent oxyfluoride glasses and nanocrystalline glass ceramics, *Journal of Applied Physics* 105,013516(2009)
- [9] V.B.sreedhar, D.Ramachari, C.K.Jayasankar, Optical properties of zincfluorophosphate glasses doped with Dy^{3+} ions, *Physica B* 408(2013) 158-163.
- [10] Xin-yuan Sun, Shi-ming Haung, Xiao-san Gong, Qing-chun Gao, Zi-piao Ye, Chun-Yan Cao, Spectroscopic properties and simulation of white –light in Dy^{3+} -doped silicate glass, *Journal of Non-Crystalline Solids* 356(2010) 98-101.
- [11] K.Siva Rama Krishna Reddy, K.Swapna, Sk.Mahamuda, M.Venkateswarlu, A.S.Rao, G.Vijya prakash, investigation on structural and luminescence features of Dy^{3+} ions doped alkaline-earth boro telluride glasses for optoelectronic devices, *Opt. Mat* 85(2018)200-210.
- [12] Agata Gorny, Marta soltys, Joanna Pisarska, Wojciech A.Pisarski, Spectroscopy and energy transfer in lead borate glasses doubly doped with Tm^{3+} and Dy^{3+} ions, *Spectrochimica Acta, Part A: Molecular, and Biomolecular Spectroscopy* 192 (2018) 140-145.
- [13] A.Ichoja, S.Hashim, S.K.Ghosal, I.H.Hashim, R.S.Omar, Physical and structural studies on magnesium borate glasses doped with dysprosium ion, *Journal of Rare earths* 2018.
- [14] Nsha Deopa, Shubham Saini, Sumandeep Kaur, Aman Prasad, A.S.Rao, Spectroscopic investigations on Dy^{3+} ions doped zinc lead alumina borate glasses for photonic device application, *Journal of Rare earths* 2018.
- [15] RajyasreeCh, Krishna Rao D, Spectroscopic investigations on alkali earth bismuth borate glasses doped with CuO. *J Non Cryst Solid* 357, (2011) 836–41.
- [16] L. Balachander, G. Ramadevudu, Md. Shareefuddin, R. Sayanna, Y.C. Venudhar, IR analysis of borate glasses containing three alkali oxides, *ScienceAsia* 39 (2013): 278–283.
- [17] Ritu Sharma, A.S.Rao, Photoluminescence on Dy^{3+} ions doped zinc lead tungsten Tellrite glasses for optoelectronic devices, *J.Non-cryst. Solid.* 495(2018)85-94.
- [18] L.VijayaLakshmi, K.Naveenkumar, K.Srinivasa Rao, Pyung Hwang, Bright up-conversion white light emission from Er^{3+} doped lithium fluoro zinc borate glasses for photonic applications, *J.Molecular Structure*, 1155(2018) 394-402.
- [19] Rungsan Ruamnikhom, Patarawagee Yasaka and Jakrapong Kaewkhao, Physical and optical properties of Dy^{3+} bismuth barium borate glasses, *J.Thai interplinary Research*, 12(2017)1-4.
- [20] A.S. Rao, Ahammed, Y.N., Reddy, R.R., and Rao, T.V.R., Spectroscopic Studies of Nd^{3+} - doped alkali fluoro-boro-phosphate glasses, *Opt. Mater.*, 10 (1998) 245 – 252.
- [21] Y.C. Ratnakaram and Reddy, A.V., Electronic spectra and optical band gap studies in neodymium chloro-phosphate glasses, *J. Non-Cryst. Solids*, 277 (2000)142 – 154.
- [22] K.Liganna, Ch.SrinivasaRao, C.K.Jayasanka, Optical properties and generation of white light in Dy^{3+} - doped phosphate glasses, *J.Quantitative Spectroscopy & Radiative Transfer* 118(2013) 40-48.
- [23] S.A.Saleem, BC.Jamalaiah, M.Jayashimhadr, A.Srinivas Rao, Kiwn Jang, L.Rama Moorthy, Luminescence studies of Dy^{3+} ion in alkali lead tellurofluoroborate glasses, *J.Quantitative Spectroscopy & Radiative Transfer* 112(2011)78-84.